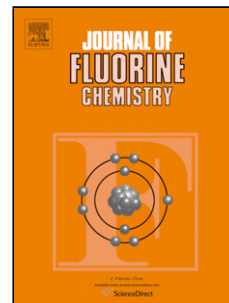


Journal Pre-proof

Systematic Elucidation of Crystal Structure of Fluorinated Gemini-Type Diamide Derivatives Having Different Lengths with Thixotropic Induced-Ability to Solvents

Haruka Maruyama, Keito Fukushi, Rei Okano, Eiichi Satou, Tomoko Yajima, Atsuhiko Fujimori



PII: S0022-1139(20)30056-7
DOI: <https://doi.org/10.1016/j.jfluchem.2020.109505>
Reference: FLUOR 109505

To appear in: *Journal of Fluorine Chemistry*

Received Date: 27 November 2019
Revised Date: 29 February 2020
Accepted Date: 3 March 2020

Please cite this article as: Maruyama H, Fukushi K, Okano R, Satou E, Yajima T, Fujimori A, Systematic Elucidation of Crystal Structure of Fluorinated Gemini-Type Diamide Derivatives Having Different Lengths with Thixotropic Induced-Ability to Solvents, *Journal of Fluorine Chemistry* (2020), doi: <https://doi.org/10.1016/j.jfluchem.2020.109505>

This is a PDF file of an article that has undergone enhancements after acceptance, such as the addition of a cover page and metadata, and formatting for readability, but it is not yet the definitive version of record. This version will undergo additional copyediting, typesetting and review before it is published in its final form, but we are providing this version to give early visibility of the article. Please note that, during the production process, errors may be discovered which could affect the content, and all legal disclaimers that apply to the journal pertain.

© 2019 Published by Elsevier.

Systematic Elucidation of Crystal Structure of Fluorinated Gemini-Type Diamide Derivatives Having Different Lengths with Thixotropic Induced-Ability to Solvents

Haruka Maruyama,^a Keito Fukushi,^b Rei Okano,^c Eiichi Satou,^c Tomoko Yajima,^d

Atsuhiko Fujimori^{b,*}

^a *Faculty of Engineering, and ^b Graduate School of Science and Engineering, Saitama University, 255 Shimo-okubo, Sakura-ku, Saitama 338-8570, Japan*

^c *R & D Dept. Laboratory Additive Unit, Kusumoto Chemicals Ltd., 4-18-6, Benten, Soka-shi Saitama, 340-0004, Japan*

^d *Department of Chemistry, Faculty of Science, Ochanomizu Univ, Bunkyo-ku, Tokyo, 112-8610, Japan*

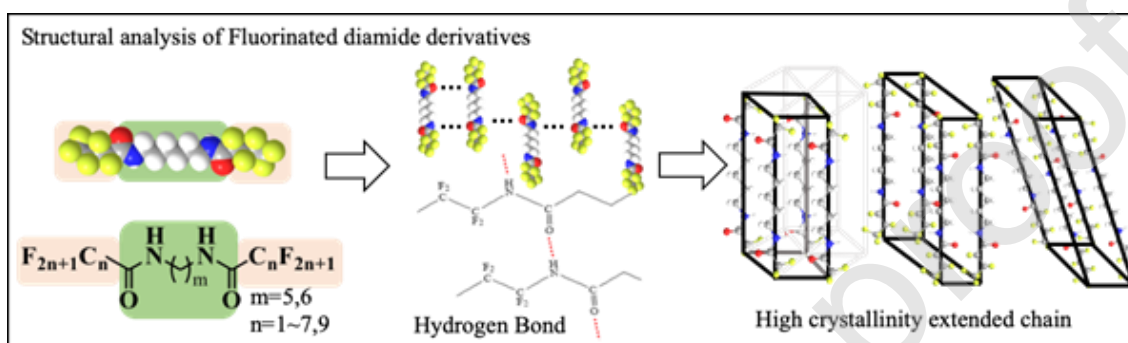
*Corresponding Author

Tel. and Fax: +81 48 858 3503

E-mail address: fujimori@apc.saitama-u.ac.jp

Graphical Abstract

H. Maruyama, et al



Highlight

- Fluorinated Gemini-type diamide derivatives with different length were systematically synthesized.
- Crystal structure of fluorinated diamides were systematically analyzed.
- Fluorinated diamides used in this study formed extended chain crystals.
- Almost all fluorinated diamides formed monoclinic packing.
- Fluorinated diamides used in this study indicated gelation ability of solvents.

ABSTRACT

Molecular packing structures for Gemini-type diamide derivatives with different linker and fluoroalkyl chain lengths were systematically determined using reciprocal lattice analysis.

Diamide derivatives with two fluorocarbons, in which the linker was replaced with one

hexamethylene chain and one pentamethylene chain, exhibited hydrogen bonding and crystallinity. Powder X-ray diffraction profiles displayed extremely sharp diffraction peaks like inorganic materials. Small-angle X-ray scattering analysis indicated extended chain crystals (ECCs) in these molecular groups. Reciprocal lattice analysis and high crystallinity allowed for the development of packing models for all compounds used in this study. Fifteen compounds were assigned to nearly orthorhombic and/or slightly distorted monoclinic systems, with one exception. All fluorinated Gemini-type diamides are characterized by a developed *c*-axis and have an *ab*-plane area that can accommodate a fluorocarbon chain. These fluorinated Gemini-type diamide derivatives are candidates for additive molecules to induce solvent thixotropy and form crystalline nanofibers through intermolecular hydrogen bonding. A correlation was found between molecular chain packing and crystal growth; a helical growth mode that permits gel formation by incorporating solvent molecules was also confirmed.

Keywords: Gemini-type diamides; fluorocarbons; crystalline packing; reciprocal lattice analysis; thixotropic molecules

1. Introduction

Recently, the behavior exceeding the hierarchy, from the microscopic molecular level to beyond the mesoscopic form to the macroscopic physical properties, is called the "cooperative phenomenon" [1]. These phenomena are not easily predicted by technology. On the sub-nanometer level, molecular groups can aggregate [2], orient [3], and integrate [4], in specific patterns to create micrometer-scaled morphologies with physical properties that can be studied at the millimeter-to-meter scale. However, the physical properties and functionality measured on this scale may not account for factors other than molecular characteristics. Supramolecular chemistry [5] represents one approach to studying higher-order structures [6] and physical properties of molecular groups exceeding hierarchy by organizing/assembling molecules [7, 8].

"Host-guest" compounds [9], such as crown ethers [10] and cyclodextrins [11], are well-known in classical supramolecular chemistry for their ability to contain molecules and ions via intermolecular interactions. Liquid crystals [12], organic crystals [13], Langmuir-Blodgett (LB) films [14-17], self-assembled films [18], and biomolecular structures [19], are also regarded as supramolecules. In addition, liposomes [20] and micelles [21], used in drug delivery systems [22], are considered to be supramolecules. Supramolecules can form from various forces, including van der Waals interactions (which are enhanced by molecular

arrangements) [23], hydrogen bonding [24], π - π interactions [25], and CH- π interactions [26], all of which are capable of long-range interactions [27].

Multiple molecular functions can be induced using the supramolecular super-hierarchical [28] cooperative effect. These attractive effects, such as liquid crystallinity [29], chirality [30], light emission properties [31], magnetism [32], polarization [33], mechanical properties [34], water/oil repellency [35, 36], and transparency/light propagation properties [37, 38], stem from the properties of molecular groups. The phenomenon of gelation [39] often results from hydrogen bond networks formed between solvated molecules [40]. Thixotropy can result from similar forces [41]. Thixotropy can be defined as an increase in viscosity over time [42]. Using molecular technology, sponge-like gel structures trap solvent molecules, mainly through fiber entangling via hydrogen-bond-induced molecular organization [43]. Because hydrogen bonds are easily broken by applied external forces, the morphological structure disintegrates and the solvent can flow freely [44]. When this behavior is reproduced under static conditions, thixotropy is achieved by the additive molecule [45].

When used for industrial applications, this technology will not only increase viscosity, but will require the surrounding solvent to be gelled or solidified. Additional applications may be possible for gelation and thixotropy as well. For example, it may be possible to create multitasking thixotropic additive molecules by introducing functional sites that induce hydrogen bonding. Importantly, all molecular functions are derived from structure. However,

the unique function of a multifunctional molecule is difficult to predict unless the aggregate structure spontaneously formed by the molecular group can be analyzed. We studied diamide-based Gemini-type thixotropic additive molecules that are also used as anti-drip agents for automotive paints. The corresponding molecule is modified with fluorocarbon to ensure that the paint has thixotropic properties and is water- and oil-repellent (to promote a clean painted surface). Since fluorocarbons are dispersible in nonpolar solvents [46], new thixotropic agents have been developed with a wide choice of solvents. Moreover, the use of such paints on watercraft could prevent the adherence of barnacles, which stick firmly to the hull and promote pollution. Conventionally, a 2:1 condensed diamide derivative comprising 12-hydroxystearic acid and a hexamethylenediamine that contains an asymmetric carbon has been used as a thixotropic agent. Entanglement of the helical nanofibers via hydrogen bonding controls the incorporation of solvent molecules. Over-developed fibers induce contamination on the paint surface and lead to a nonuniform appearance due to visible light scattering. Thus, it is important to control the physical properties derived from the structures formed by thixotropic molecules [47-50].

In this study, we performed reciprocal lattice analysis [51] of wide-angle X-ray diffraction data for precise analysis of the structure responsible for this function. This technique can effectively obtain molecular packing using a powder or thin film sample without requiring a single crystal [52]. As there are few examples of detailed structures of

aggregates of fluorine-based low-molecular compounds, this study contributes to our understanding of solid structures for the molecular group (Fig. 1).

2. Materials and methods

2.1. Synthesis of fluorinated Gemini-type diamide derivatives with different chain lengths

Figures 2 (a) and (b) show the compounds used in this study. Diamide derivatives having one pentamethylene linker and two fluorocarbons with chain lengths C_nF_{2n+1} ($n = 1-7$) and having one hexamethylene linker and two fluorocarbons with chain length C_nF_{2n+1} ($n = 1-9$), were used. The former and the latter are designated $2F_nC_5$ -diamides and $2F_nC_6$ -diamides, according to their chain lengths, respectively. Schemes 1(a) and (b) describe the synthesis of the compounds used in this study using linker starting materials pentamethylenediamine and hexamethylenediamine, respectively. Three equivalents of methyl fluorinated long chain carboxylate was added to tetrahydrofuran (THF) solvent at 0 °C for 1 h to obtain the compound. After the reaction, compounds were purified by column chromatography, and target compounds were obtained in 79–98% yield. Synthesis was confirmed by nuclear magnetic resonance spectroscopy (NMR). Furthermore, recrystallization was performed using THF and hexane, and high purity compounds were obtained.

The reason for the comparative selection between the hexamethylene and the pentamethylene linkers is to evaluate whether the orientation of the amide group has any effect. Many of the diamide-based thixotropic additives that have been practically used conventionally are those having a hexamethylene linker. Even from experimental facts, molecules with short linkers are disadvantageous for expressing gelation ability. In this study, in order to verify the odd-even effect of the linker length, we used a group of compounds with different linker lengths. Detailed chemical structure analysis data including ^1H NMR, ^{13}C NMR, ^{19}F NMR, etc. are shown in Supporting Information.

2.2. Hydrogen bonding and the solid-state structures of fluorinated Gemini-type diamide derivatives

Infrared (IR) spectroscopy was performed with all synthesized compounds (Bruker AXS Tensor II) to evaluate the formation of hydrogen bonding. For transmission measurements, 32 scans were accumulated using the KBr disk method. In addition, wide-angle X-ray diffraction (WAXD) was measured to evaluate the crystal structure and crystallinity of each sample (Bruker AXS D8 Advance, $\text{CuK}\alpha$ radiation, 40 kV, 100 mA). The apparatus was equipped with a rotating anode source and a two-dimensional semiconductor detector for high power measurement. Further, higher-order structural analysis was conducted using small-angle X-ray scattering (SAXS, Rigaku Nanoviewer, $\text{CuK}\alpha$ radiation, 40 kV, 40 mA). Similarly, this

instrument was equipped with a rotating anode source and a two-dimensional semiconductor detector. To elucidate molecular packing, reciprocal lattice analysis was performed with the WAXD data. The lattice constant of stearic acid [53] or polytetrafluoroethylene [54] was used as the initial value for calculations.

2.3. Gelation, thixotropy, and nanofiber morphology of fluorinated Gemini-type diamide derivatives

Gelation tests were performed using ethanol, hexane and benzene solvents. For each solvent, fluorinated Gemini-type diamide derivative was introduced as a thixotropic additive at 1 wt%. The solution was warmed to 80 °C, then cooled to room temperature once the additive was dissolved. The gelled sample was dried and the xerogel was observed using a scanning electron microscope (SEM, Hitachi SU8030 ultrahigh resolution field emission SEM). In addition, a spin-cast film was prepared from a 9:1 solvent mixture of xylene/ethanol, and detailed morphological observations were made using an atomic force microscopy (AFM, SII SPA300 with SPI3800 probe station, Dynamic Force Mode, Si tip with spring constant 1.5 N / m).

3. Results and Discussion

Figure 3 shows IR spectra of fluorinated Gemini-type diamide derivatives with different lengths and linkers. In these spectra, C-F stretching vibrations are observed equally at approximately 1000–1200 cm^{-1} , and a carbonyl band is observed at 1700 cm^{-1} . The broad band around 2350 cm^{-1} is derived from carbon dioxide, though to a varying degree. One critical feature in the spectra of these derivatives is the presence of an amide band around 3200–3300 cm^{-1} . This absorption band is isolated: there is no hydrogen bonding band for a free amide around 3700 cm^{-1} . Thus, the spectra indicate that hydrogen bonding networks lead to the structure observed for each derivative.

Figure 4 shows WAXD profiles of fluorinated Gemini-type diamide derivatives with different lengths and linkers. What can be seen at a glance is that all compounds display high crystallinity based on the occurrence of very sharp diffraction peaks. Many of the compounds display periodic structure developed on the low-angle side. For example, compounds other than 2F₉C₆ and 2F₅C₅-diamides etc. show sharp, high-intensity diffraction peaks at low angles. This indicates that it has a structure developed in the *c*-axis direction. 2F₉C₆ and 2F₅C₅-diamides have relatively low intensity diffraction peaks and are wide, but all diffraction lines can be indexed. In this case, d_{100} , d_{111} , d_{120} (2F₉C₆-diamide), or d_{010} , d_{110} , d_{111} (2F₅C₅-diamide) strongly reflects the order of crystal planes existing relatively in the *ab*-plane. On the other hand, the d_{002} planes, which are weak but corresponds to the order in the *c*-axis direction, is confirmed in both profiles. Since long-chain compounds are easy to orient,

many compounds show a structure developed in the c-axis direction, but some substances may remain relatively isotropic. By the way, in general, amphiphiles and/or polymers having long fluorocarbons tend to exhibit strong diffraction peaks derived from the distance between two-dimensional fluorocarbons (around 5.0 Å). Here, clear diffraction peaks were observed from approximately $d = 4.4$ to 4.7 Å. For hydrocarbon compounds, this spacing narrows to around 4.1 to 4.2 Å. In low molecular weight compounds composed of light elements, the diffraction peak is clearly visible because the X-ray scattering factor for fluorine atoms is relatively large. However, the half-width of the peak indicates that these compounds are highly ordered. IR measurements suggest that regulated structure is likely based on highly developed hydrogen bonding. Due to the abundant number of sharp diffraction peaks, we used reciprocal lattice analysis to determine the systematic crystal structures and molecular packing for these fluorinated molecular groups. An accurate understanding of long-period structures is required to proceed with this analysis reliably. Therefore, higher-order structure analysis was performed for these compounds *via* SAXS measurements.

Figure 5 shows the SAXS patterns and profiles of excerpted fluorinated Gemini-type diamide derivatives with different lengths and linkers. All SAXS patterns are circular and show isotropic structures. Profiles obtained by integrating this pattern in the equatorial direction show clear long-period values. In fact, almost all of these values correspond to the extended chain length of each molecule. Thus, these fluorinated Gemini-type diamide

derivatives are extended chain crystals (ECCs). Based on this hypothesis, we have drawn a packing model by indexing the WAXD diffraction peaks and applying reflection to the reciprocal space. All the samples used in this study had a single melting point and were analyzed as single-phase crystals at a measurement temperature 23 °C. This assumption is the premise of the structural analysis in this study.

Figures 6, 7, and 8 show packing models for fluorinated Gemini-type diamide derivatives by reciprocal lattice analysis. In particular, Figure 6 shows the crystal structure of compounds with a pentamethylene linker and a fluorocarbon chain 1–6 carbon atoms long. Of the 15 compounds used in this study, only 2F₁C₅-diamide could not be assigned using the initial value referred to lattice constant for amphiphilic low molecular weight compounds. In this case, the most appropriate initial value was the hexagonal packing of polytetrafluoroethylene before a phase transition at room temperature. As a result, this compound alone has a lattice structure comprising a rhombus-shaped unit cell composed of two isosceles triangles. The *a*- and *b*-axes lengths are 5 Å, and the lattice constant is close to that of a Teflon polymer. Since the molecular chain is short, we propose that a lattice structure is formed in which the degree of rotation freedom of molecular chains is allowed at isotropic molecular chain packing positions. On the other hand, the *c*-axis length is extremely developed.

Although $2F_2C_5$ - and $2F_3C_5$ -diamides are both assigned to orthorhombic systems, packing similar to the hexagonal crystal assignment for $2F_1C_5$ -diamide results when different initial values are used in the calculations. The unit cell is rectangular, but the difference in lattice distortion is small and the shape is anisotropic. In both cases, the b -axis is relatively long, but the a -axis is about 5 Å. The a -axis had similar values for all compounds used in this study. In addition, these materials are converged to an extreme developed structure along the c -axis. The $2F_4C_5$ -, $2F_5C_5$ - and $2F_6C_5$ -diamides are attributed to monoclinic packing with slightly reduced symmetry. Many of the packing structures of the compounds analyzed this time were attributed to monoclinic packing. For the initial value, we used the lattice constant for the polymorphic structure of stearic acid. Regardless of chain length, there is no significant difference in the a -axis, and the b -axis is relatively long. Both have a developed structure along the c -axis. Since angle β is not a right angle, the packing structure can be drawn with inclination. As the chain length increases, in-plane interactions between the helical fluorocarbon chains slightly increases, and a tilted molecular chain array forms.

Figure 7 shows the crystal structure of $2F_7C_5$ -diamide, and $2F_nC_6$ -diamide at $n=1-4$ with hexamethylene linker. $2F_7C_5$ -diamide has the shortest a -axis length among pentamethylene linker compounds and the anisotropy of unit cell is high. The c -axis becomes longer as the molecular chain length increases and is the longest among the pentamethylene linker compounds. The above seven compounds show relatively similar packing even if their crystal

systems are different, and the unit cell changes from isotropic to anisotropic arrangement as the chain length increases, and lattice symmetry decrease. On the other hand, almost all packing model of compounds with hexamethylene linkers assign to the monoclinic system. In this figure, 2F₁C₆-, 2F₃C₆- and 2F₄C₅-diamides are assigned to monoclinic packing. Since exceptionally only 2F₂C₅-diamide forms orthorhombic packing, slightly high symmetric packing appears to be achieved with relatively short chain lengths in these like materials. The systematic resemblance of the *a*-axis length, the extension of the *b*-axis length to the *a*-axis one, and the structure that is highly developed in the *c*-axis direction, including 2F₅C₆- to 2F₉C₆-diamides, show similar trends (Fig. 8).

The above results are summarized in Fig. S1 in the Supporting Information. It can be seen that most of the structures are described by monoclinic packing, except for those of some of the short-chain compounds. This lattice forms mainly from hydrogen bonds between amide groups. However, since the extended chain-like packed structure has aligned molecular phases, it is expected that the relatively weak van der Waals forces between fluorocarbons will be enhanced. This enhancement of van der Waals interactions between fluorocarbons likely distorts the lattice, leading to packing with vertical conformation and high symmetry for the short chain compounds. Interestingly, this tendency tends to be higher for pentamethylene compounds than for hexamethylene compounds. Since relatively strong van der Waals forces exist between hydrocarbon chains, the lateral affinity is stronger for

hexamethylene compounds, thus they are more likely to produce more distorted lattices [55, 56]. As a result, the lattice packing of fluorinated Gemini-type diamide derivatives is predicted to be hexagonal or orthorhombic with vertical chain conformation if intermolecular hydrogen bonding alone is observed. As the hydrocarbon chain length increases, the strength of the two-dimensional affinity slightly distorts the lattice and tends to converge to monoclinic packing. In addition, these compounds form ECCs and develop periodic structures along the *c*-axis, while the *ab*-plane creates a wide, anisotropic in-plane structure that can easily accommodate thicker fluorocarbon chains of about 5 Å or more.

Table 1 shows the results of representative gelling tests with these compounds. The thixotropic additives used in this study are intended to be applied and commercialized to paints for private vehicles. The types of paints include aqueous solvents, phenyl solvents, alcohol solvents, and normal alkane solvents. Ethanol, hexane, and benzene used in this study are limited in their use due to their volatility and toxicity, but can be regarded as standard solvents for the above paint-based solvents. Comparing compounds with the same fluorocarbon length but different linker lengths, it can be seen that gelation ability with phenyl solvents is high. This tendency was observed for toluene and xylene, as well as benzene. On the other hand, pentamethylene compounds were able to gel hexane, a nonpolar solvent. Hexamethylene compounds did not gel hexane but were able to gel alcohol. As the chain length increases, solvent gelation ability is difficult to observe. Perhaps the pore size in

which these thixotropic additive molecules are fibrillated and entangled by hydrogen bonding must match the size of the solvent molecule [49]: it may be difficult to create a pore size that can easily incorporate large solvent molecules. Phenyl-type solvents are likely to be taken into the intertwined fiber structure, due to their relatively large molecular size. Results indicate that hexamethylene compounds can grow fibers even in polar solvents, but that longer fluorocarbon chain lengths seem to lower solubility and cause precipitation. Thus, the molecular size and solubility of the solvent appear to be a factor in the selectivity of solvent gelation. In addition, all of the solvents that showed gelation also displayed thixotropic properties; they flowed again when stimulated by a magnetic stirrer and re-gelled after a lapse of time. This suggests that relatively weak hydrogen bonds are responsible.

Figure 9 shows a SEM image of nanofibers formed by a fluorinated diamide derivative gelled with a benzene solvent. In this sample, the obtained benzene gel was dried and observed as a xerogel. Almost all molecules that caused gelation displayed fibrous forms as xerogels, but $2F_2C_5$ - and $2F_3C_5$ -diamides, whose crystal structure was attributed to orthorhombic crystals, were particularly mixed, with many helical fiber forms. A $2F_3C_5$ -diamide film was prepared by spin-casting and AFM was also conducted. A straight fiber containing a partly spiral shaped fiber was observed. Helical morphology tends to occur when molecules are packed more densely. In this study, the analyzed crystal lattice and fiber sizes are disparate, but they may be influenced by the hyper-hierarchical cooperation effect [57].

Fibers with spirals tend to entangle efficiently, and solvent gelation tends to be more efficient.

These results are summarized in Fig. 10. In this study, molecular packing in the crystal structure of fluorinated diamide derivatives with solvent thixotropic ability was systematically shown. In future studies, we plan to clarify the correlation between molecular packing and gelation.

4. Conclusions

Reciprocal lattices of fluorinated Gemini-type diamide derivatives with different fluorocarbon and linker lengths were systematically analyzed to evaluate their molecular packing. Diamide derivatives with hexamethylene and pentamethylene linkers form hydrogen bonding networks and display high crystallinity. The compounds form ECCs, which develop along the *c*-axis. Reciprocal lattice analysis revealed packing arrangements for all 15 synthesized compounds. Except for some short-chain compounds, the majority of compounds were assigned to the monoclinic system. Intermolecular hydrogen bonding is the main interaction forming the crystal lattice, while van der Waals interactions between long fluorocarbons likely cause the distortion that slightly reduces the lattice symmetry.

Fluorinated Gemini-type diamide derivatives demonstrated gelation ability similar to that of a general-purpose solvent. Several fluorothixotropic agents were able to gel phenyl solvents with large molecular sizes. Gelation results indicate solvent selectivity as well. Fluorinated

Gemini-type diamide derivatives with relatively dense packing tend to form helical fibers when solvated. Since the helical form promotes gelation, future elucidation of molecular packing and helical form is worthwhile.

Declaration of Interest Statement

There is no conflict of interest for this paper

Acknowledgements

This study was supported by JSPS KAKENHI Scientific Research on Innovative Areas “MSF Materials Science (Grant Numbers JP 19H05118)”, and JSPS KAKENHI Grant Numbers (C) JP 17K05988.

[References and Notes]

1. S.N. Dorogovtsev, A.V. Goltsev, J.F.F. Mendes, Critical phenomena in complex networks, *Rev. Mod. Phys.* 80 (2008) 1275-1335.
2. A.K. Boal, F. Ilhan, J.E. DeRouchey, T. Thurn-Albrecht, T.P. Russell, V.M. Rotello, Self-assembly of nanoparticles into structured spherical and network aggregates, *Nature*. 404 (2000) 746-748.
3. L. Zang, Y.K. Che, J.S. Moore, One-Dimensional Self-Assembly of Planar pi-Conjugated Molecules: Adaptable Building Blocks for Organic Nanodevices, *Acc. Chem. Res.* 41 (2008) 1596-1608.
4. A. Ulman, Formation and Structure of Self-Assembled Monolayers, *Chem. Rev.* 96 (1996) 1533-1554.
5. M.C. Daniel, D. Astruc, Gold nanoparticles: Assembly, supramolecular chemistry, quantum-size-related properties, and applications toward biology, catalysis, and nanotechnology, *Chem. Rev.* 104 (2004) 293-346.
6. A.L. Ankudinov, B. Ravel, J.J. Rehr, S.D. Conradson, Real-space multiple-scattering calculation and interpretation of x-ray-absorption near-edge structure, *Phys. Rev. B.* 58 (1998) 7565-7576.
7. O. Ikkala, G. ten Brinke, Functional materials based on self-assembly of polymeric supramolecules, *Science*. 295 (2002) 2407-2409.

8. G. Decher, Fuzzy nanoassemblies: Toward layered polymeric multicomposites, *Science*. 277 (1997) 1232-1237.
9. K. Hirose, A practical guide for the determination of binding constants, *J. Incl. Phenom. Macrocycl. Chem.* 39 (2001) 193-209.
10. M.E. El-Khouly, O. Ito, P.M. Smith, F. D'Souza, Intermolecular and supramolecular photoinduced electron transfer processes of fullerene-porphyrin/phthalocyanine systems, *J. Photochem. Photobiol.* 5 (2004) 79-104.
11. Y. Okumura, K. Ito, The polyrotaxane gel: A topological gel by figure-of-eight cross-links, *Adv. Mater.* 13 (2001) 485.
12. L. Perez-Garcia, D.B. Amabilino, Spontaneous resolution under supramolecular control, *Chem. Soc. Rev.* 31 (2002) 342-356.
13. A. Priimagi, G. Cavallo, P. Metrangolo, G. Resnati, The Halogen Bond in the Design of Functional Supramolecular Materials: Recent Advances, *Acc. Chem. Res.* 46 (2013) 2686-2695.
14. G.L. Gaines, *Insoluble monolayers at liquid gas interfaces*, Wiley, New York (1966).
15. K. Blodgett, Monomolecular films of fatty acids on glass, *J. Am. Chem. Soc.* 56 (1934) 495-495.
16. M.C. Petty, *Langmuir-Blodgett films*, Cambridge Univ. Press, New York, (1996).
17. A. Ulman, *An Introduction to Ultrathin Organic Films: from Langmuir-Blodgett to Self-*

- assembly. Academic Press, Boston 1991.
18. H. Lee, S.M. Dellatore, W.M. Miller, P.B. Messersmith, Mussel-inspired surface chemistry for multifunctional coatings, *Science*. 318 (2007) 426-430.
19. U.Essmann, L. Perera, M.L. Berkowitz, T. Darden, H. Lee, L.G. Pedersen, A Smooth Particle Mesh Eward Method, *J. Chem. Phys.* 103 (1995) 8577-8593.
20. D.J. Ahn, E.H. Chae, G.S. Lee, H.Y. Shim, T.E. Chang, K.D. Ahn, J.M. Kim, Colorimetric reversibility of polydiacetylene supramolecules having enhanced hydrogen-bonding under thermal and pH stimuli, *J. Am. Chem. Soc.* 125 (2003) 8976-8977.
21. D.J. McMahon, B.S. Oommen, Supramolecular structure of the casein micelle, *Int. J. Dairy Sci.* 91 (2008) 1709-1721.
22. L. Li, X. Li, X.P. Ni, X. Wang, H.Z. Zi, K.W. Leong, Self-assembled supramolecular hydrogels formed by biodegradable PEO-PHB-PEO triblock copolymers and alpha-cyclodextrin for controlled drug delivery, *Biomaterials*. 27 (2006) 4132-4140.
23. K.H. Kim, S. Lee, C.K. Moon, S.Y. Kim, Y.S. Park, J.H. Lee, J.W. Lee, J. Huh, Y. You, J.J. Kim, Phosphorescent dye-based supramolecules for high-efficiency organic light-emitting diodes, *Nat. Commun.* 5 (2014) 4769.
24. O. Ikkala, G. ten Brinke, Hierarchical self-assembly in polymeric complexes: Towards functional materials, *ChemComm.* 19 (2004) 2131-2137.
25. M.E. Zandler, F. D'Souza, The remarkable ability of B3LYP/3-21G((*)) calculations to

- describe geometry, spectral and electrochemical properties of molecular and supramolecular porphyrin-fullerene conjugates, *C. R. Chim.* 9 (2006) 960-981.
26. M. Nishio, The CH/ π hydrogen bond in chemistry. Conformation, supramolecules, optical resolution and interactions involving carbohydrates, *Phys. Chem.* 13 (2011) 13873-13900.
27. Q. Shi, R. Cao, D.F. Sun, M.C. Hong, Y.C. Liang, Solvothermal syntheses and crystal structures of two metal coordination polymers with double-chain structures, *Polyhedron.* 20 (2001) 3287-3293.
28. S. Yagai, T. Nakajima, K. Kishikawa, S. Kohmoto, T. Karatsu, A. Kitamura, Hierarchical organization of photoresponsive hydrogen-bonded rosettes, *J. Am. Chem. Soc.* 127 (2005) 11134-11139.
29. A.T.W.M. Hendriks, G. Zeeman, Pretreatments to enhance the digestibility of lignocellulosic biomass, *Bioresour. Technol.* 100 (2009) 10-18.
30. C. Janiak, Engineering coordination polymers towards applications, *Dalton Trans.* 14 (2003) 2781-2804.
31. D.J. Schlegel, D.P. Finkbeiner, M. Davis, Maps of dust infrared emission for use in estimation of reddening and cosmic microwave background radiation foregrounds, *Astrophys. J.* 500 (1998) 525-553.
32. J.B. Pendry, A.J. Holden, D.J. Robbins, W.J. Stewart, Magnetism from conductors and enhanced nonlinear phenomena, *IEEE Trans. Microw. Theory Tech.* 47 (1999) 2075-2084.

33. J.P. Perdew, Y. Wang, Accurate and simple analytic representation of the electron-gas correlation energy, *Phys. Rev. B.* 45 (1992) 13244-13249.
34. C. Lee, X.D. Wei, J.W. Kysar, J. Hone, Measurement of the elastic properties and intrinsic strength of monolayer graphene, *Science.* 321 (2008) 385-388.
35. W. Barthlott, C. Neinhuis, Purity of the sacred lotus, or escape from contamination in biological surfaces, *Planta.* 202 (1997) 1-8.
36. A. Tuteja, W. Choi, M.L. Ma, J.M. Mabry, S.A. Mazzella, G.C. Rutledge, G.H. McKinley, R.E. Cohen, Designing superoleophobic surfaces, *Science.* 318 (2007) 1618-1622.
37. K.S. Kim, Y. Zhao, H. Jang, S.Y. Lee, J.M. Kim, K.S. Kim, J.H. Ahn, P. Kim, J.Y. Choi, B.H. Hong, Large-scale pattern growth of graphene films for stretchable transparent electrodes, *Nature.* 457 (2009) 706-710.
39. P. Terech, R.G. Weiss, Low molecular mass gelators of organic liquids and the properties of their gels, *Chem. Rev.* 97 (1997) 3133-3159.
40. S. Kitagawa, R. Kitaura, S. Noro, Functional porous coordination polymers, *Angew. Chem. Int. Ed.* 43 (2004) 2334-2375.
41. H.A. Barnes, Thixotropy - A review, *J.Non-Newton Fluid.* 70 (1997) 1-33.
42. J. Mewis, N.J. Wagner, Thixotropy, *Adv. Colloid Interface Sci.* 147-48 (2009) 214-227.
43. Y. Zhang, R.G. Weiss, How do H-bonding interactions control viscoelasticity and thixotropy of molecular gels? Insights from mono-, di- and tri-hydroxymethylated

- alkanamide gelators, *J. Colloid Interface Sci.* 486 (2017) 359-371.
44. H.W. Gao, R.J. Yang, J.Y. He, L. Yang, Rheological Behaviors of PVA/H₂O Solutions of High-Polymer Concentration, *J. Appl. Polym. Sci.* 116 (2010) 1459-1466.
45. V. Boffa, J.E. ten Elshof, D.H. A. Blank, Preparation of templated mesoporous silica membranes on macroporous alpha-alumina supports via direct coating of thixotropic polymeric sols, *Microporous Mesoporous Mater.* 100 (2007) 173-182.
46. H. Machida, Y. Abiko, S. Hirayama, Q. Meng, S. Akasaka, A. Fujimori, Correlation Between Nanodispersion of Organo-Modified Nanodiamond in Solvent and Condensed Behavior of Their Organized Particle Films, *Colloids Surf. A.* 562 (2019) 416-430.
47. M. Iizuka, Y. Nakagawa, K. Ohmura, E. Satou, A. Fujimori, Two-dimensional Growth of Crystalline Nanofiber Fabricated from Gemini-type Amphiphilic Diamide Derivative Inducing the Thixotropic Property, *J. Colloid Interf. Sci.* 498 (2017) 64-75.
48. M. Iizuka, Y. Nakagawa, Y. Moriya, E. Satou, A. Fujimori, Comparison of Structure/Function Correlational Property of Three Kinds of Gemini-type Thixotropic Surfactants Capable of Forming Crystalline Nanofiber Based on Hydrogen Bonding – Solid-state Structure, Two-dimensional Molecular Film Forming, and Epitaxial Growth Behavior–, *Bull. Chem. Soc. Jpn.* 91 (2018) 813-823.
49. Y. Nakagawa, K. Watahiki, E. Satou, Y. Shibasaki, A. Fujimori, Elucidation of the Origin of Thixotropic Inducing Properties of Additive Amphiphiles, and the Creation of a High-

- Performance Triamide Amphiphile, *Langmuir*. 34 (2018) 11913-11924.
50. Y. Nakagawa, K. Watahiki, R. Okano, E. Satou, Y. Shibasaki, A. Fujimori,
Structure/Function Correlation of Thixotropic Additives Based on Three Leaf-like
Triamide Derivatives containing Three Alkyl-Chains, *Colloids Surf. A*. 575 (2019) 27-41.
51. H. Jagodzinski, H.P. Klug, L.E. Alexander, X-ray Diffraction Procedures for
Polycrystalline and Amorphous Materials, second ed., Wiley, New York, 1974.
52. M.A. Neumann, X-Cell: a novel indexing algorithm for routine tasks and difficult cases, *J.
Appl. Crystallogr.* 36 (2003) 356-365.
53. C.A. Sperati, H.W. Starkweather Jr, Fluorine-containing polymers. II.
Polytetrafluoroethylene, *Adv. Polym. Sci.* 2 (1961) 465-495.
54. E.Von Sybow, On the Structure of Crystal form B of Stearic Acid, *Acta Cryst.* 8 (1955)
557-560.
55. A. Fujimori, T. Araki, H. Nakahara, E. Ito, M. Hara, H. Ishii, Y. Ouchi, K. Seki, In-Plane
X-ray Diffraction and Polarized NEXAFS Spectroscopic Studies on the Organized
Molecular Films of Fluorinated Amphiphiles with Vinyl Groups and Their Comb-
Polymers, *Chem. Phys. Lett.*, 349 (2001) 6-12.
56. A. Fujimori, Y. Shibasaki, T. Araki, H. Nakahara, Monolayer Assemblies of Comb
Polymers Containing Different Kinds of Fluorocarbon Side-Chains, *Macromol. Chem.
Phys.*, 205 (2004) 843-854.

57. J.F. Letard, L. Capes, G. Chastanet, N. Moliner, S. Letard, J.A. Real, O. Kahn, Critical

temperature of the LIESST effect in iron (II) spin crossover compounds, Chem. Phys.

Lett., 313 (1999) 115-120.

Journal Pre-proof

[SCHEME and TABLE TITLES]

Scheme 1. Synthetic process for the compounds used in this study: (a) pentamethylene and (b) hexamethylene derivatives.

[FIGURE CAPTIONS]

Figure 1. Research strategy of this study.

Figure 2. (a) Diamide derivatives having one pentamethylene linker and two fluorocarbons with chain length C_nF_{2n+1} ($n = 1-7$) and (b) diamide derivatives having one hexamethylene linker and two fluorocarbons with chain length C_nF_{2n+1} ($n = 1-9$).

Figure 3. IR spectra of fluorinated Gemini-type diamide derivatives with different lengths and linkers.

Figure 4. WAXD profiles of fluorinated Gemini-type diamide derivatives with different lengths and linkers.

Figure 5. SAXS patterns and profiles of excerpted fluorinated Gemini-type diamide derivatives with different lengths and linkers.

Figure 6. Schematic illustration of packing models for fluorinated Gemini-type diamide derivatives (compounds with a pentamethylene linker and a fluorocarbon chain of length 1-6) by reciprocal lattice analysis.

Figure 7. Schematic illustration of packing models for fluorinated Gemini-type diamide

derivatives ($2F_7C_5$ -diamide, and $2F_nC_6$ -diamide at $n = 1-4$ with hexamethylene linker) by reciprocal lattice analysis.

Figure 8. Schematic illustration of packing models for fluorinated Gemini-type diamide derivatives ($2F_nC_6$ -diamide at $n = 5-9$ with hexamethylene linker) by reciprocal lattice analysis.

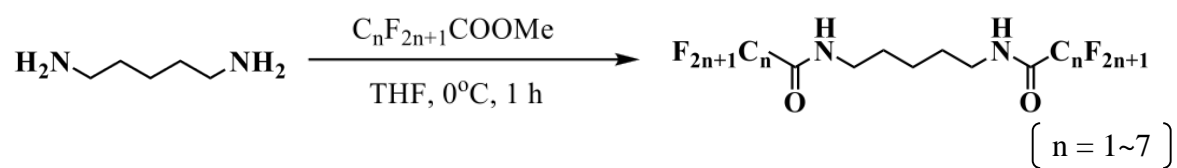
Figure 9. SEM images of xerogels and AFM image of spin-cast film of fluorinated Gemini-type diamide derivatives.

Figure 10. Schematic illustration of concluding remarks in this study.

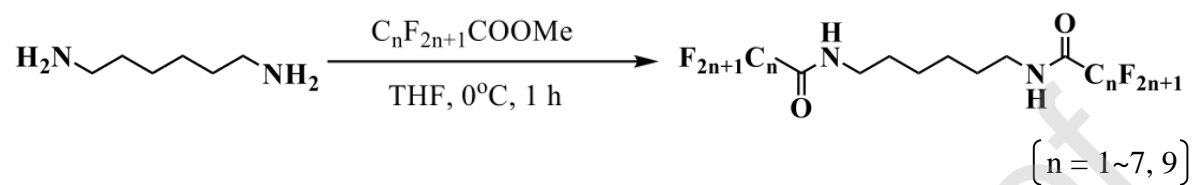
Scheme 1

H. Maruyama, et al

(a)



(b)



Journal Pre-proof

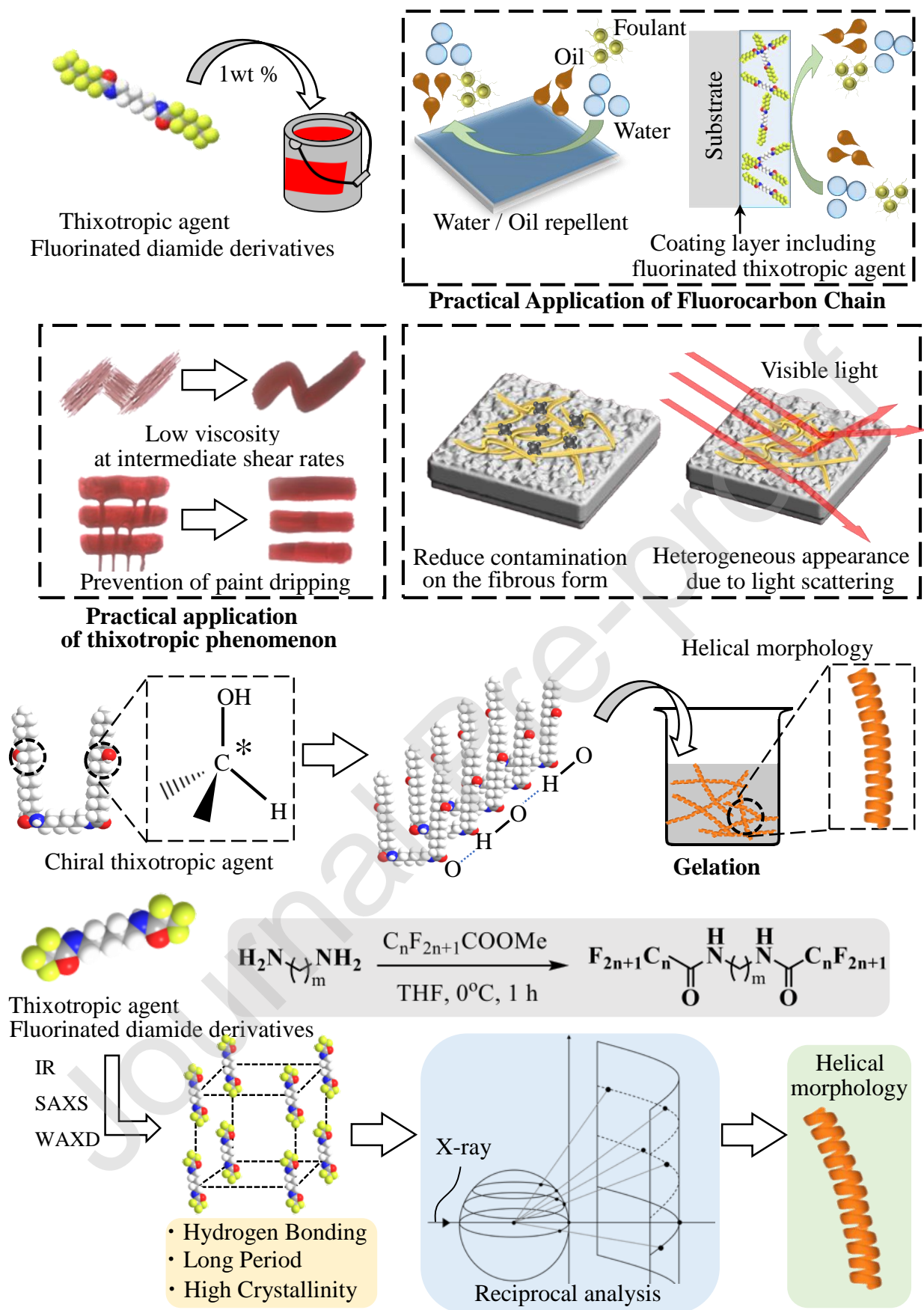


Figure 1

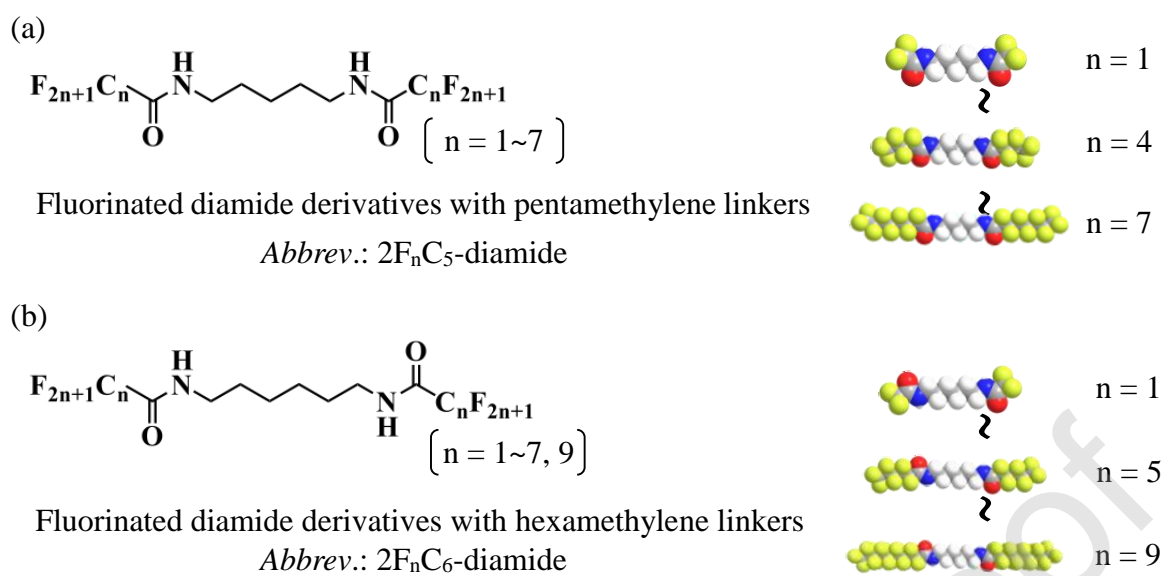


Figure 2

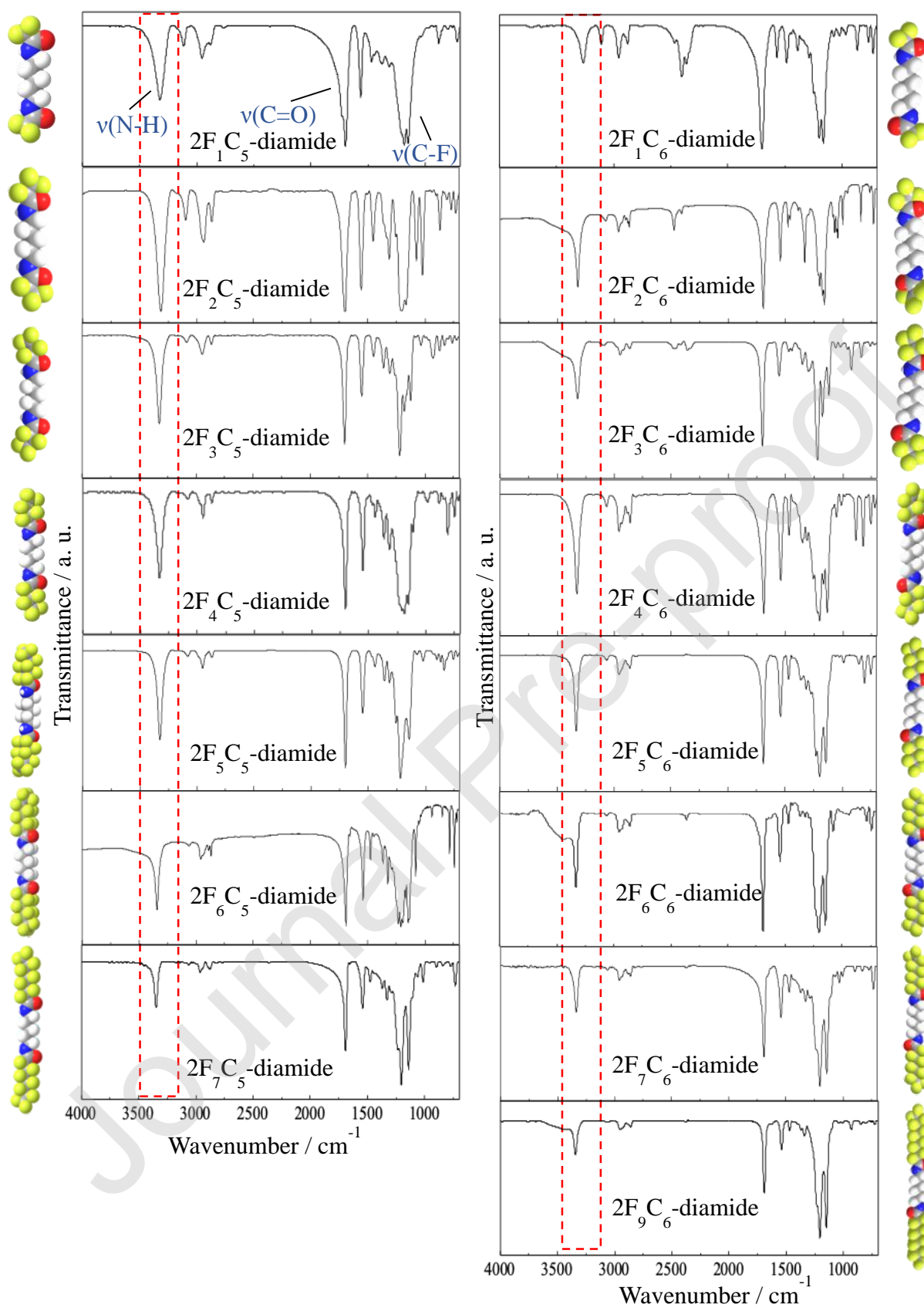


Figure 3

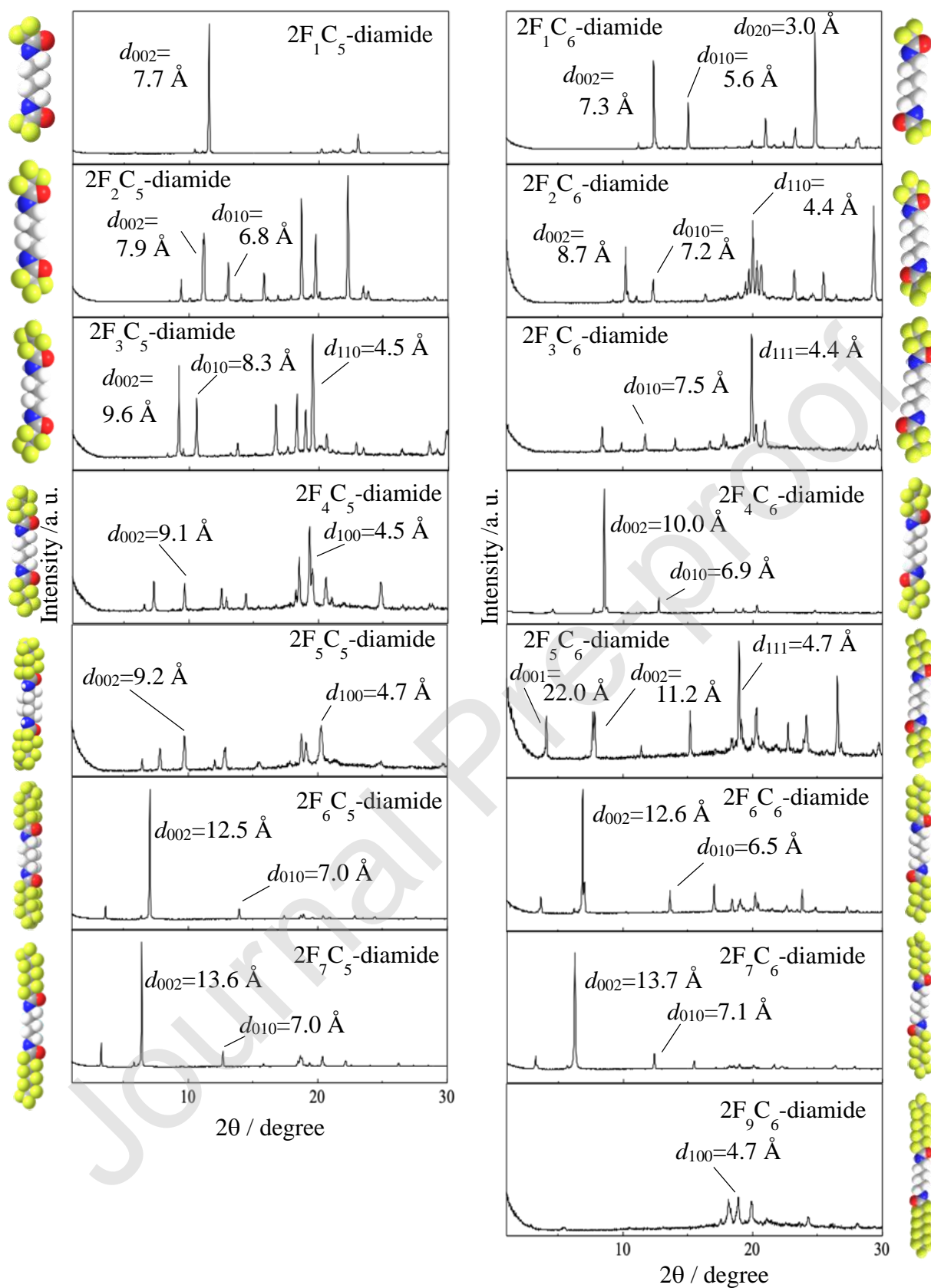


Figure 4

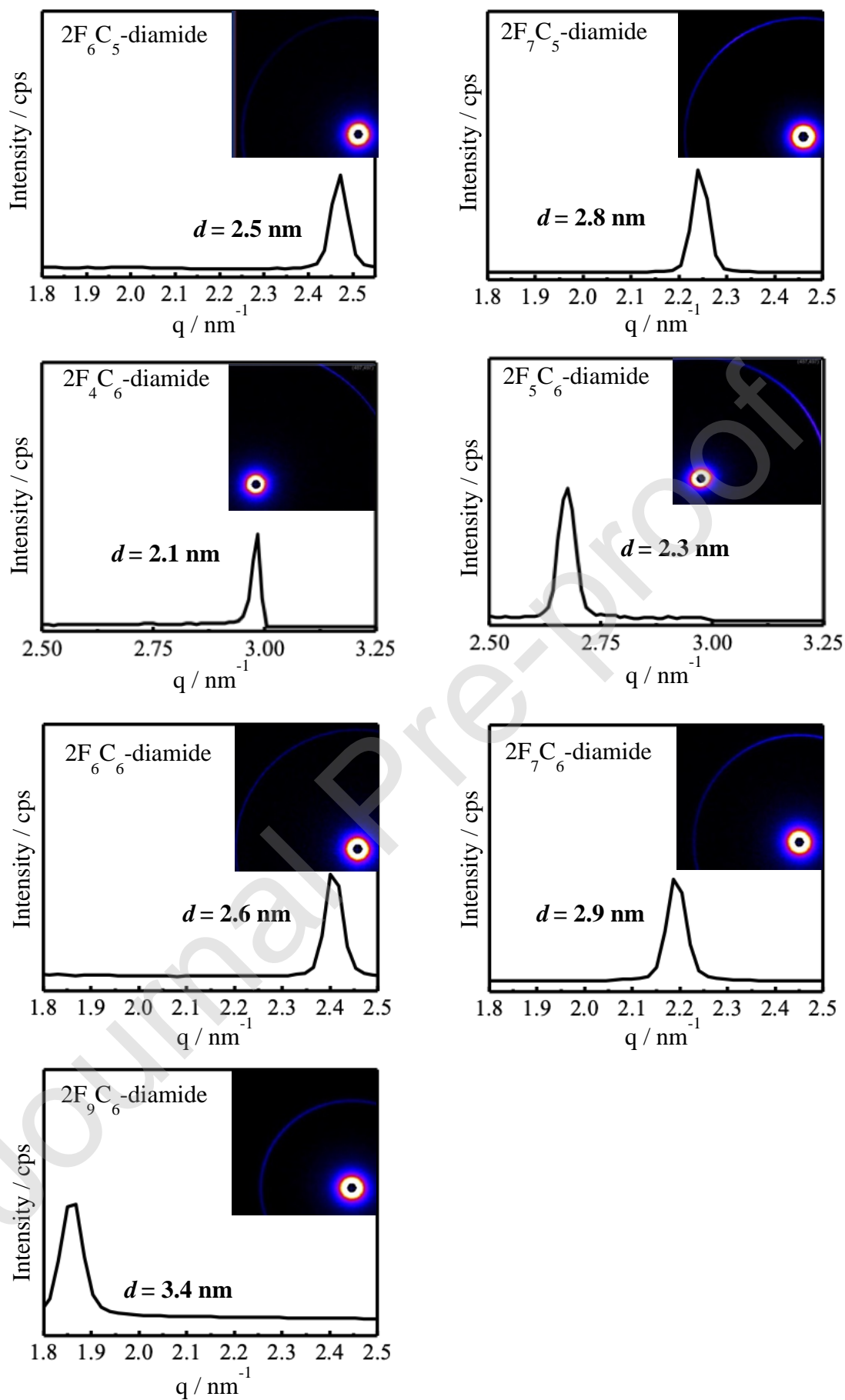


Figure 5

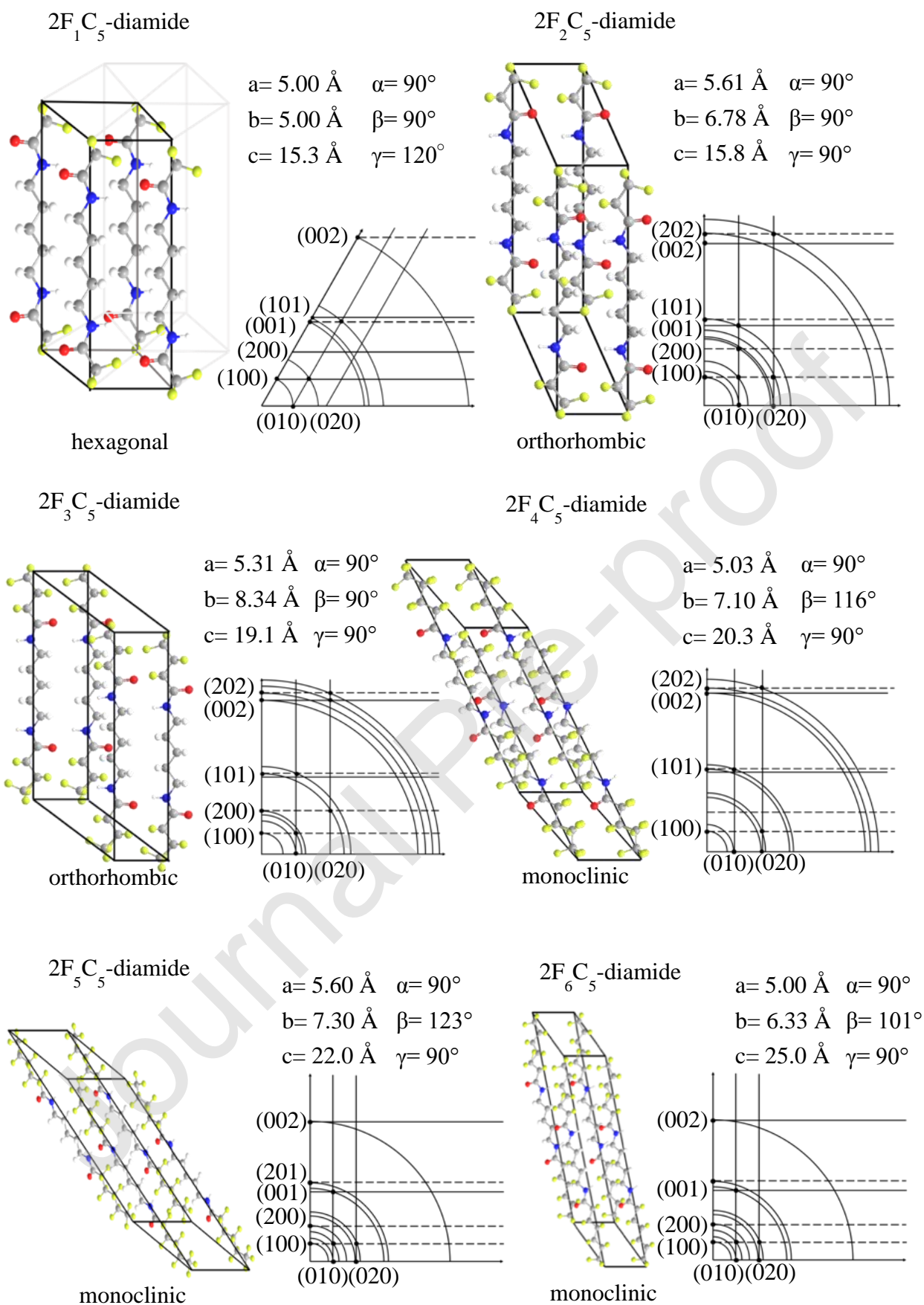


Figure 6

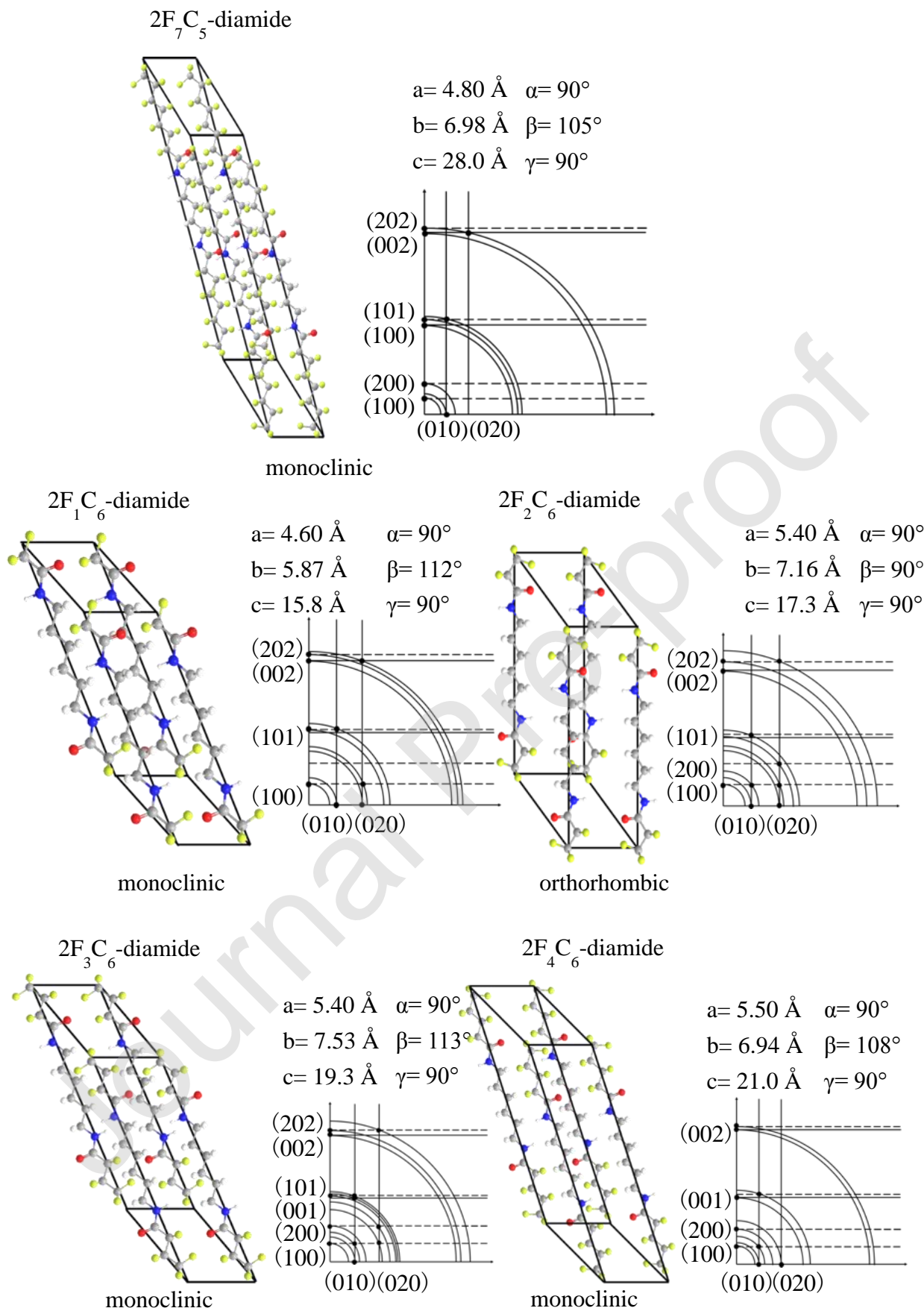


Figure 7

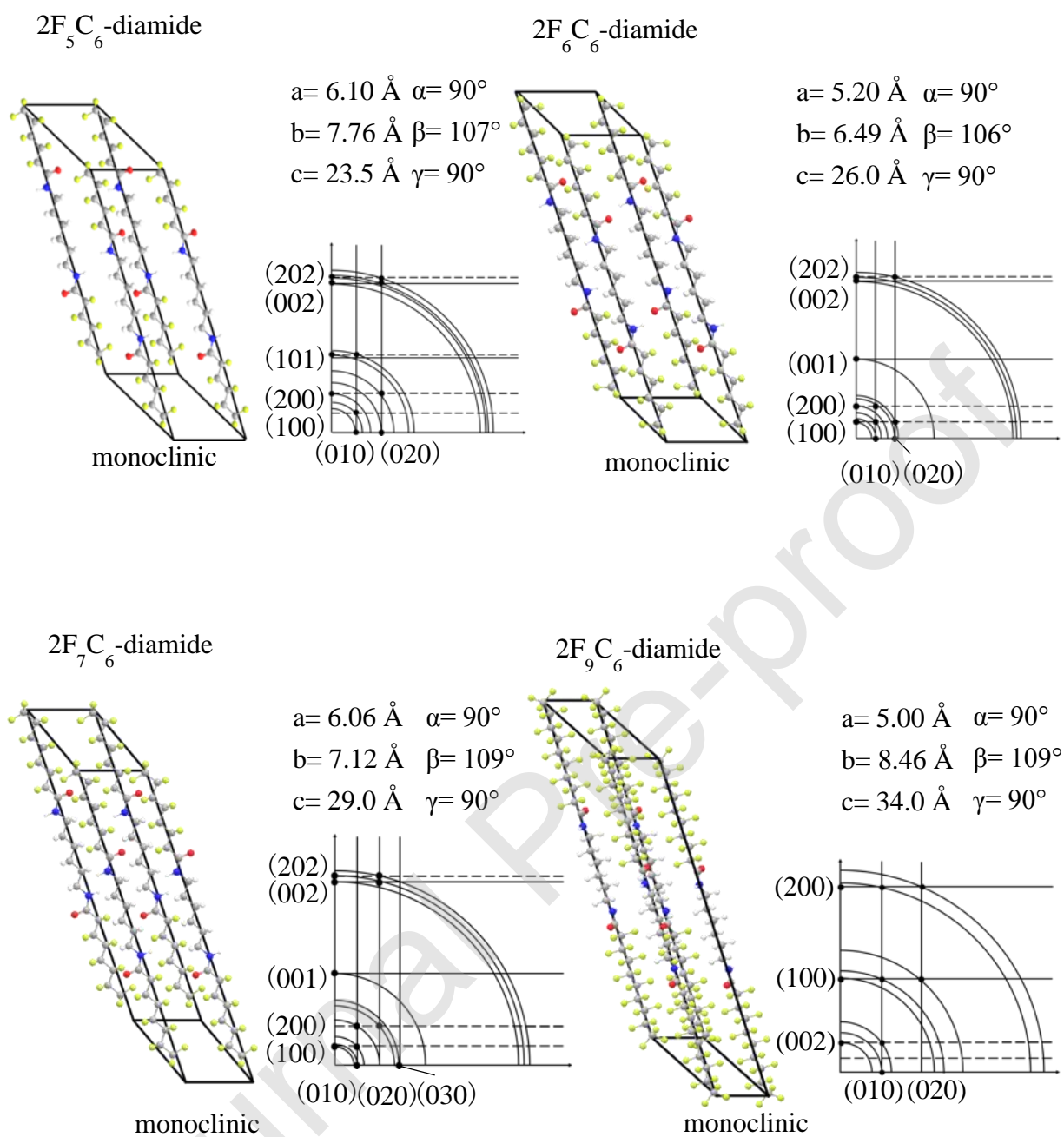


Figure 8

H. Maruyama, et al

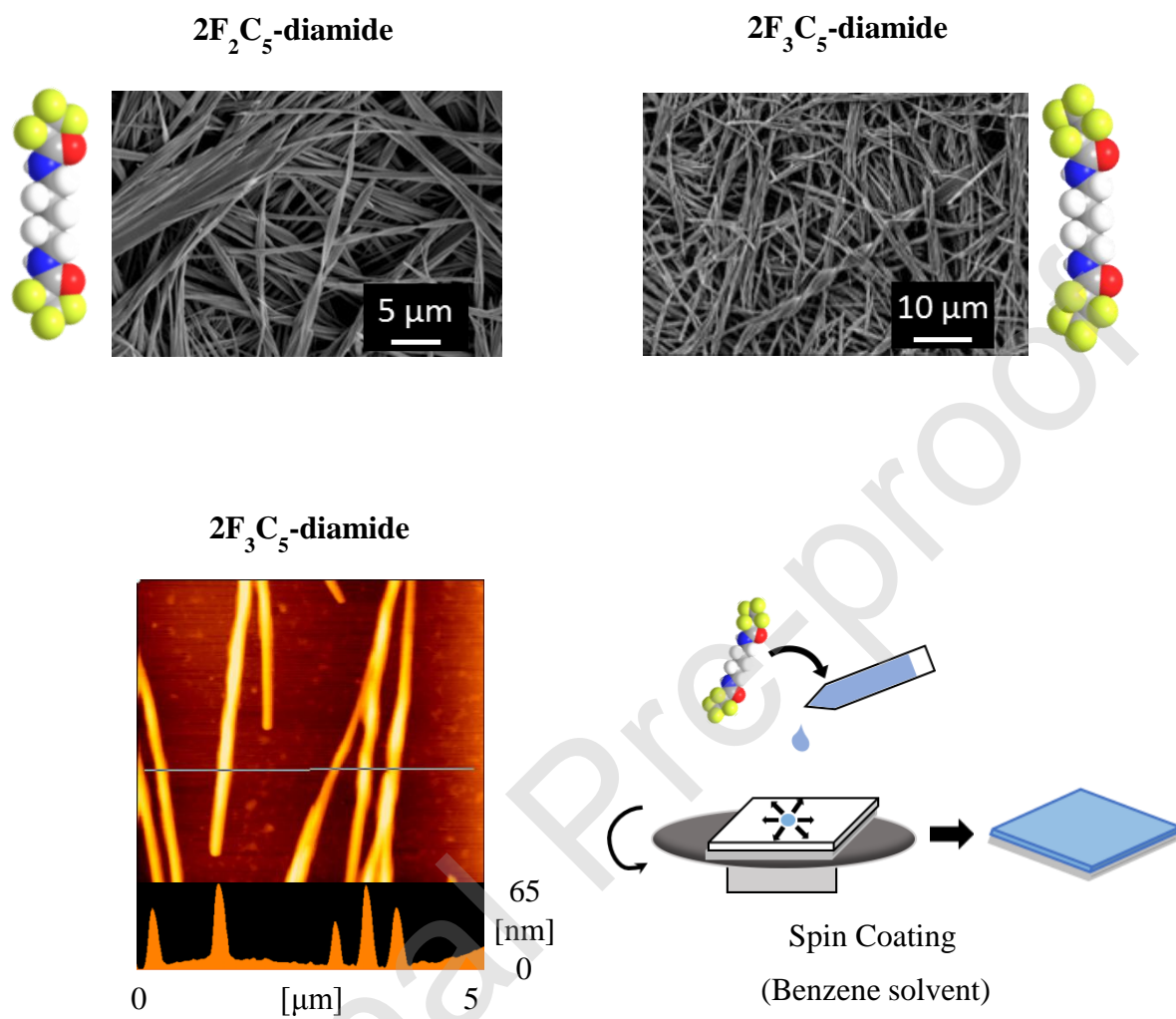


Figure 9

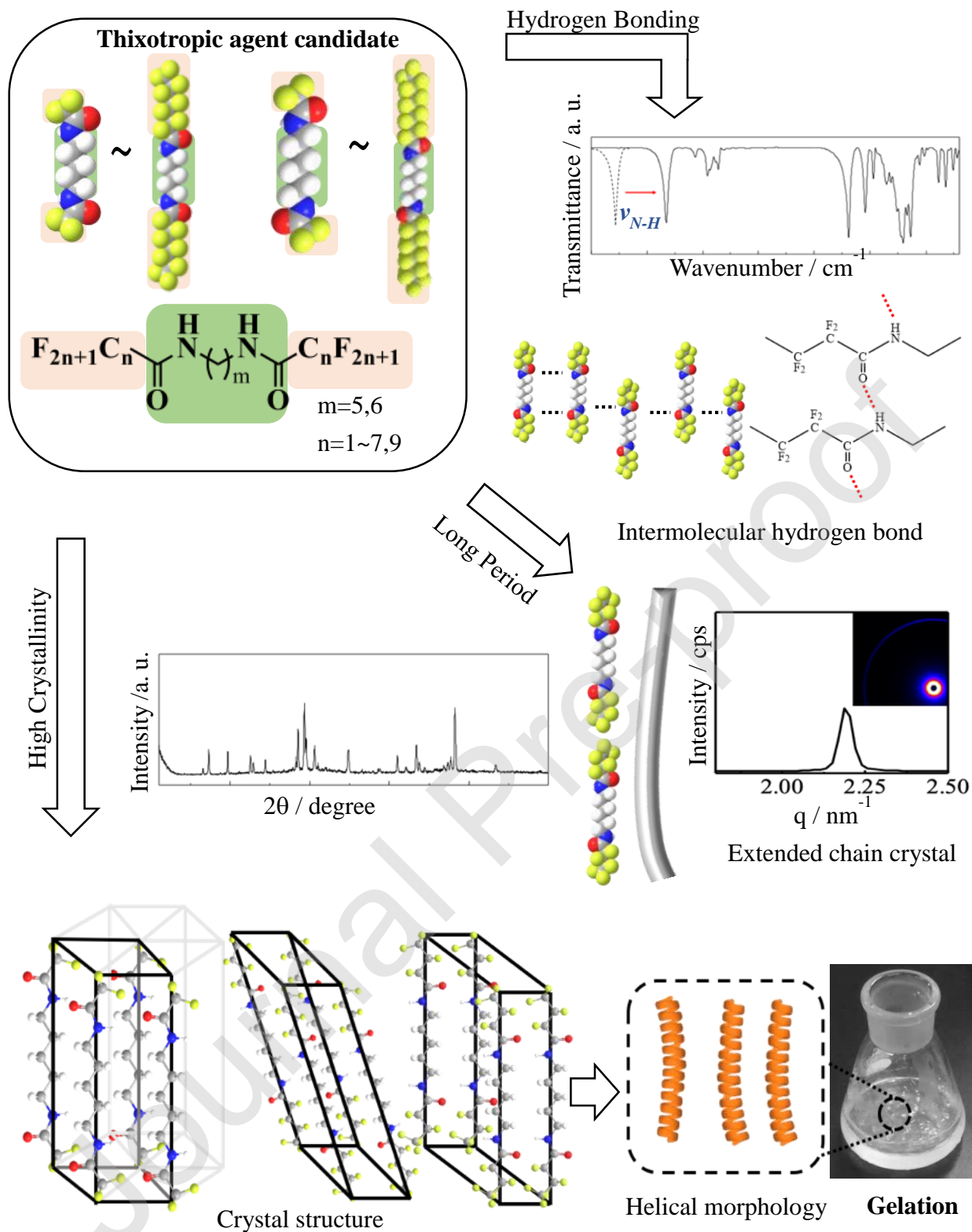


Figure 10

Table 1. Results of gelation test for several solvents including fluorinated Gemini-type diamide derivatives as thixotropic additives.

Sample	Solvent		
	Ethanol	Hexane	Benzene
2F ₄ C ₅ -diamide	solution	gelation	gelation
2F ₄ C ₆ -diamide	gelation	solution	gelation
2F ₉ C ₆ -diamide	precipitation	solution	solution

※solution: no gelation/maintaining of solution state

※precipitation: occurrence of precipitation